

1 **Title:** On the protective role of the blood vessels in glaucomatous damage: a transversal
2 study

3

4 **Authors (last name, first name):**

5 Cánovas-Serrano, Yaiza¹(ycanovas@alu.ucam.edu), corresponding author; Vallés-San-
6 Leandro, Lorenzo²(lorenzo.valles@gmail.com); Rodríguez-Izquierdo, Miguel
7 Ángel²(rodriguez@vistaircovision.com); Lajara-Blesa, Jerónimo^{2,3} (jlajara@ucam.edu);
8 López-Serrano, Rafael⁴(rafael.lopez@um.es);

9

10 **Affiliations:**

11 ¹ Health Sciences PhD program, Catholic University of Murcia (UCAM), Campus de los
12 Jerónimos nº135, Guadalupe 30107, Murcia, Spain.

13 ² Clinical Research Department, Vista Ircovisión, Murcia, Spain.

14 ³ Faculty of Health Sciences, Catholic University of Murcia (UCAM), Spain.

15 ⁴ Faculty of Economics, University of Murcia (UMU), Spain.

16 **Corresponding Author:**

17 Name: Yaiza Cánovas-Serrano

18 Email: ycanovas@alu.ucam.edu

19 **NOTE:** This preprint reports new research that has not been certified by peer review and should not be used to guide clinical practice.
Address: Campus de los Jerónimos nº 135

20 Guadalupe 30107, Murcia, Spain.

21

22 **Abstract**

23 **Purpose:** To corroborate whether vessels on the surface of the optic nerve head can
24 provide protection against the loss of underlying axons in subjects with manifest
25 glaucoma.

26 **Methods:** In this pilot study, thirty-six glaucomatous eyes with a perimetric defect in the
27 Bjerrum area were included. The retinal nerve fiber layer (RNFL) thickness was
28 measured in each of the sectors of the clock-hour map obtained by Cirrus HD-OCT
29 considering the presence or absence of blood vessels. These sectors were related with
30 their corresponding areas of the retina examined in the visual field using a mathematical
31 model of the retina introduced by Jansonius, in order to determine the values of threshold
32 sensitivity in those areas in the presence or absence of vessels.

33 **Results:** We corroborated the protective role of the blood vessel for peripapillary RNFL
34 thickness of clock-hour 12 despite obtaining a p-value ($p = 0.023$; $w = 228.5$) close to the
35 acceptance zone ($p \geq 0.05$). The mean \pm standard deviation with vessel and without vessel
36 were 70.95 ± 24.35 and 88.46 ± 23.96 , respectively. No differences were found between
37 the mean values of threshold sensitivity to the presence or absence of blood vessels in
38 each of the sectors considered.

39

40 **Conclusions:** Our findings do not allow us to affirm that there is an association between
41 the presence of a vessel and protection against glaucomatous damage in subjects with an

42 advanced manifestation of the disease. In the future, more extensive studies are needed
43 to study this relationship in subjects with early glaucoma.

44 **Key words:** astrocytes, visual field, primary open-angle glaucoma, aqueous humor,
45 blood vessel.

46

47 **Introduction**

48 Glaucoma is a multifactorial progressive optic neuropathy in which elevated intraocular
49 pressure (IOP) is a strong risk factor [1]. The structural changes that occur during the
50 development of the disease are well-defined [2], unlike its etiology, which still remains
51 uncertain today.

52 The insufficient explanation of the pathogenesis of glaucoma by mechanical and vascular
53 theory raises interest in the permeability of the optic nerve making way for a new
54 hypothesis that name the existence of posterior aqueous humor flow could be a possible
55 cause of glaucoma [3]. That explains and defines the structural changes that have occurred
56 in the development of the disease to achieve its detection as early as possible, thanks to
57 the incorporation and improvement of imaging diagnostic devices [4-7] without having
58 to wait to the functional manifestations of the visual field, in which case the loss of nerve
59 fibers is irreversible and of great amount [8].

60 There is a fourth posterior pathway through which part of the aqueous humor leaves the
61 eye, through the vitreous and the retina, without entering the anterior chamber. This is
62 due to the lack of an epithelial barrier on the anterior surface of the vitreous. When there
63 is an increase in resistance in the regulation of the aqueous humor outflow normal
64 pathway with an increase in IOP, these discontinuities or holes produce an increase in
65 aqueous humor flow toward the posterior pole [9]. This process is supported by the
66 existence of optic nerve head (ONH) permeability, since the nerve`s vitreous interface is

67 formed by astrocytes, where fenestrations are described that allow the free passage of
68 fluid and solutes from the vitreous to prelaminar tissue [10, 11]. These astrocytes are
69 united to each other and to the extracellular matrix, among others, by adherent junctions
70 rich in N-cadherine, a calcium dependent adhesion molecule. These types of unions are
71 characterized by allowing the passage of water and small molecules, which confer a
72 permeability to the ONH [9]. When the aqueous humor, poor in calcium, passes through
73 the optic nerve and comes into contact with astrocytes, it produces a separation of the
74 adherent junctions due to a drop in calcium concentrations in these junctions. This would
75 produce a rupture of the membrane junctions between the astrocytes and cause their
76 destruction, allowing the introduction of the aqueous humor into the extracellular spaces
77 of the optic nerve [11,12]. Do not forget that astrocytes are considered as essential
78 elements for protecting axons of the optic nerve [3].

79 This new hypothesis, which is defended in the present study, should explain the loss of
80 axons in conditions of high or low IOP and account for the initial or early damage of
81 glaucoma in the ONH as a consequence of the deviation of the aqueous humor outlet
82 during the development of glaucoma toward the posterior pole, in which there is
83 protective role played by the blood vessel covering the underlying axons [3, 9].

84 This new postulate would allow determining the pattern of visual field loss because the
85 scotomas would be limited in their extent by the projection of the blood vessels in the
86 visual field [9,11,12]. Being possible to carry out a detection as early as possible, through
87 the techniques of perimetric and morphological data, to adopt the appropriate therapeutic
88 measures.

89 There are mathematical models that can be used to predict the location and progression
90 of scotomas in glaucoma. We propose to use the Jansonius model [13,14], based on
91 photographic images of the retina, to relate structural and functional injury. The area of

92 the papilla covered by the central vessels of the retina corresponded to the delimited
93 papillary border by dividing the optic nerve into sectors generated by OCT. While the
94 Jansonius algorithm determines the area of the retina where the dendritic trees of the
95 ganglion cells are located.

96 The objective of the present study is to confirm, in patients affected by glaucomatous
97 visual field damage, whether the presence of a blood vessel on the surface of the ONH
98 provides protection against the progressive destruction of underlying axons.

99

100 **Methods**

101 **Study participants**

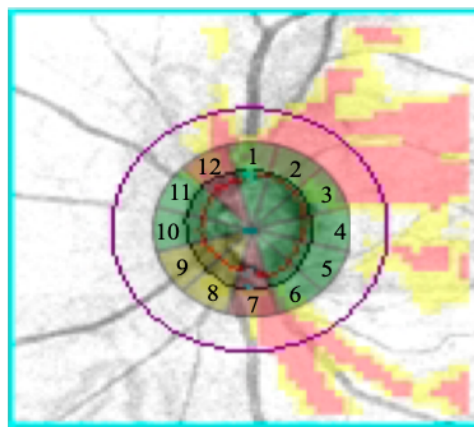
102 This was a cross-sectional study. All subjects were recruited from the hypertension
103 consultation at the Vista-Ircovisión ophthalmological center, in Murcia between May
104 2018 and September 2018.

105 All subjects underwent a full ophthalmic examination: a review of clinical history, best-
106 corrected visual acuity, slit-lamp biomicroscopy, intraocular pressure measurement by
107 applanation tonometry, automated perimetric- visual field assessment with Octopus 600
108 (Bloss, software version 3.6.1. Haag-Streit, Switzerland) and peripapillary analysis using
109 optical coherence tomography (OCT) with Cirrus HD-OCT (Carl Zeiss Meditec, Inc.,
110 Dublin, CA; software version: 6.0.2.81) based on spectral domain (SD) technology using
111 the Optic Disc Cube 200x200 protocol.

112 The inclusion criteria for both normal subjects and glaucoma patients were age > 18 years
113 old, no history of retinal disease or optic nerve disease including non-glaucomatous optic
114 neuropathy, ocular surgery, diabetes mellitus, hypertension and refractive error < 5
115 diopters of sphere or 3 diopters of cylinder. Glaucoma subjects were included if they had
116 a definitive diagnosis of visual field damage in the Bjerrum area.

117 **Study protocol**

118 The ONH parameters that were analyzed were RNFL thickness of all 12 clock-hour
119 sectors listing them clockwise in the right eye and counterclockwise in the left eye. The
120 presence or absence of a blood vessel, in each of the sectors studied in the peripapillary
121 region, was done by superimposing the clock-hour map on the fundus photograph
122 obtained with OCT (Fig. 1).



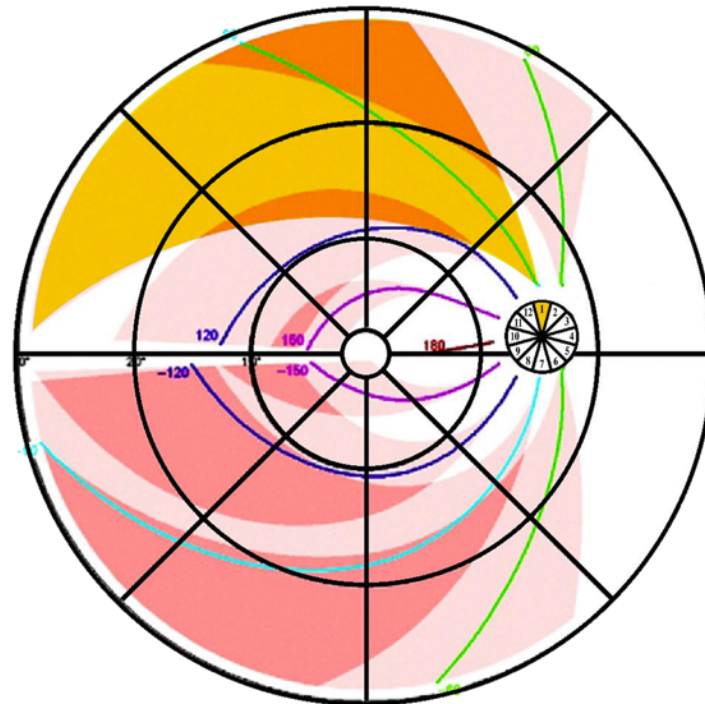
123

124 **Figure 1.** Superimposition of the clock-hour map onto the fundus photography of the
125 optic nerve with Cirrus-HD. We observe the presence of blood vessels at clock-hour 1, 7,
126 8, 9 and 11 in a patient diagnosed with glaucoma.

127

128 In order to obtain threshold sensitivity values, the mathematical retinal model of
129 Jansonius (2009) [13] was used to connect the bundle of nerve fibers of a certain region
130 of the retina examined by the visual field with the corresponding area of input of that
131 bundle of fibers in the peripapillary region of the optic nerve. Jansonius (2009) [13]
132 introduced a mathematical model for describing the nerve fiber bundle trajectories of the
133 human retina. To do this, we adapted the clock-hour map within the determined position
134 of the optic nerve in the Jansonius model (2009) [13] matching each fiber bundle with
135 each of the 12 sectors of the clock-hour map, thus obtaining our own proposed model to
136 relate the structural and functional damage (Fig. 2). The threshold sensitivity value per

137 sector was obtained by projecting each bundle of Jansonius nerve fibers onto the visual
138 field examination considering the inversion that needed to be made (the nasal hemiretina
139 was evaluated by the temporal visual field, the temporal hemiretina was evaluated by the
140 nasal visual field, the superior hemiretina was evaluated by the inferior visual field and
141 the inferior hemiretina was evaluated by the superior visual field).



142
143 **Figure 2.** Adaptation of the clock-hour map to the mathematical retina model of
144 Jansonius (2009). It is observed how each nerve fiber bundle trajectory in the human
145 retina matches to the corresponding individual clock-hour sector of the ONH (the whole
146 12 clock-hours). An example is shown of the correspondence made in the right eye
147 between the trajectory of the bundle axons along the retina according to Jansonius
148 (indicated in yellow) and its corresponding input region (clock-hour 1 in yellow) in the
149 ONH.

150

151 We calculated the mean RNFL thickness values and threshold sensitivity by stratifying
152 each of the sectors into two groups, in order to subsequently compare the glaucomatous

153 group with the presence of the blood vessel versus the glaucomatous group with absence
154 of the blood vessel in the analysis of the protective role of vessels in glaucomatous
155 damage. Similarly, previously, we measured the average values of RNFL thickness and
156 threshold sensitivity by sectors in the recruited group of control subjects to verify the
157 validation of our own proposed model. For this study, clock-hours 3, 4 and 5 were not
158 included in the statistical analysis of the variables due to the limited data obtained from
159 this area because it corresponds to the nasal side of the retina and is not affected by
160 glaucomatous injury.

161 **OCT Scanning**

162 Peripapillary ONH parameters were measured in each participant by optical coherence
163 tomography. Optic Disc Cube 200x200 protocol of Cirrus HD-OCT was used for scan
164 acquisition of the optical disc head. The protocol generates a cube of data over a 6x6 mm²
165 area centered on the optic disc by acquiring a series of 200 A-scans from 200 linear B-
166 scans (40,000 points) in about 1.5 seconds (27,000 A-scans/sec). For analysis, a built-in
167 automated algorithm identifies the center of the optic disc and places a circle of 3.46 mm
168 diameter evenly around it. After automated RNFL segmentation, the system takes
169 samples from the data cube of 256 A-scans along the path of the scan circle to obtain
170 average and sectorial (12 clock-hours) RNFL thickness. While centering and performing
171 the Cirrus-HD OCT test, patient monitoring is possible. Only good quality scans were
172 used for analysis, defined as having a signal strength greater or equal to 6 (10 =
173 maximum) without discontinuity or misalignment, involuntary saccade or blinking
174 artifacts. The parameters used for the analysis of the optic nerve head were the clock-hour
175 map and mean nerve fiber layer (NFL) thickness.

176

177 **Visual Field Testing**

178 All participants underwent the G-Program of the Octopus perimeter, TOP strategy, 30
179 central degrees, white-on-white perimetry, stimulus size III, time of exposure 100ms
180 using standard background lighting of 4 apostilbs. The visual fields were classified as
181 reliable if the reliability factor, RF, was <15%.

182 Glaucomatous visual field damage was defined based on at least 3 or more contiguous
183 depressive test points within the typical glaucoma location (Bjerrum area) with a pattern
184 deviation plot at $p < 5\%$ or a corrected standard deviation occurring in less than 5% of the
185 normal field.

186 **Statistical analysis**

187 To compare the means in the different groups, the Wilcoxon-Mann-Whitney test was
188 used. R Studio version 1.1.423 was used for statistical analysis in order to have a simple
189 way to execute the sentences of the programming language R version 3.5.0 (2018-04-23)
190 necessary to obtain the desired analyses. In all analyses, p -values < 0.05 were considered
191 significant.

192 **Results**

193 The following participants were recruited: 27 control subjects (36 eyes) and 29 patients
194 (36 eyes) diagnosed with primary open-angle glaucoma (POAG). In all, 72 patients
195 aged 50-79 years were included. The patients of the study group had been diagnosed by
196 a glaucoma specialist and were in follow-up for the disease, after having undergone the
197 functional test with at least 5 visual fields prior to their recruitment. Even so, 9 patients
198 were eliminated because the reliability limits established in the perimeter used were

199 exceeded (RF <15%). All patients had glaucomatous visual field defects (Bjerrum area)
200 and glaucoma was classified as advanced if the average value of MD = 10.25 ± 4.98
201 (≥ 6 dB). The normal control subjects presented normal perimetries and no evidence
202 of structural or functional glaucomatous damage (Table 1).

203

204 **Table 1.** Baseline characteristics of the normal control and glaucoma patients.

	Mean age (years)	MD (dB)	sLV (dB)	RFNL Average thickness (μm)
Normal	58.5 ± 6.6	-0.25 ± 1.03	1.77 ± 0.41	90.9 ± 5.4
Glaucoma	67.9 ± 9.4	10.25 ± 4.98	6.71 ± 1.85	63.7 ± 8.6

205 MD = mean defect; sLV = square loss variance; RFNL = retinal fiber layer.

206 Data are expressed as the mean \pm SD.

207

208 Regarding our work methodology, we found our regions of the visual field with their
209 corresponding sections of analysis of nerve fibers of the ONH of the hour circle by OCT,
210 when comparing our model with that used in the only study found among the bibliography
211 that performs a topographical correspondence between functional and structural tests
212 [15]. No other Jansonius-based model was found. Likewise, we found analogous with
213 other studies the mean values of nerve fiber thickness in each of the sections considered
214 (Table 2), [5,16] as well as the value of the mean visual field defect [17] both in the group
215 of subjects. control as glaucomatous patients.

216

217 **Table 2.** Peripapillary Retinal Nerve Fiber Layer Thickness (μm) of normal control and
218 glaucoma patients by location for Cirrus HD-OCT.

Parameter	Normal	Glaucoma
Sector 1	111.91 \pm 22.22	72.72 \pm 19.90
Sector 2	102.33 \pm 13.00	74.11 \pm 18.82
Sector 6	93.77 \pm 16.09	66.88 \pm 14.93
Sector 7	125.69 \pm 17.34	73.80 \pm 18.94
Sector 8	131.58 \pm 16.84	68.41 \pm 19.16
Sector 9	63.38 \pm 9.45	47.27 \pm 11.64
Sector 10	49.16 \pm 5.16	47.36 \pm 12.07
Sector 11	73.86 \pm 9.97	58.00 \pm 16.07
Sector 12	126.05 \pm 15.05	78.25 \pm 25.40

219 Data are expressed as the mean \pm SD

220

221 We can affirm that our data obtained from our analyzed sample are correct when finding
222 common analogous findings with respect to other studies. This, together with the previous
223 knowledge we have of the disease, allows us to accept as valid our proposed model to
224 match the regions of the visual field with their corresponding sectors of the optic nerve.

225 Therefore, we start from the creation of a correct model that allows us to study / analyze
226 the main objective of this work, which is to corroborate if the blood vessel really has a
227 protective role against glaucomatous lesion. We found that its influence was only
228 confirmed in section 12 of the examination of the hourly circle for the thickness of NFL
229 after the application of the WMW test, after checking the non-normality of the variables
230 involved using the Shapiro-Wilk test, confirming the rejection of equality of means (μ_1

231 = μ_2) despite the fact that the obtained value was very close to the acceptance zone ($p \geq$
 232 0.05), considering therefore the test that for this section the vessel does influence the
 233 thickness of NFL in glaucomatous subjects (Table 3).

234

Table 3. Comparison of results of mean sensitivity (dB) and peripapillary RNFL (μm) of glaucoma patients by location with vessel/without vessel.

	Glaucoma (dB)		Glaucoma (μm)	
	with vessel	without vessel	with vessel	without vessel
Sector 1	14.90 \pm 7.33	15.98 \pm 7.17	73.63 \pm 19.82	68.16 \pm 21.57
Sector 2	16.24 \pm 7.22	18.67 \pm 7.03	75.04 \pm 19.89	72.00 \pm 16.81
Sector 6	11.79 \pm 7.77	13.41 \pm 8.35	69.15 \pm 14.48	61.00 \pm 15.20
Sector 7	11.64 \pm 7.83	13.79 \pm 9.06	73.10 \pm 18.52	76.71 \pm 21.90
Sector 8	16.44 \pm 7.09	14.11 \pm 7.73	72.70 \pm 17.40	64.57 \pm 20.29
Sector 9	00.00 \pm 00.00	20.85 \pm 7.10	00.00 \pm 00.00	47.33 \pm 11.65
Sector 10	00.00 \pm 00.00	20.44 \pm 7.83	00.00 \pm 00.00	47.36 \pm 12.07
Sector 11	17.66 \pm 11.01	22.39 \pm 8.01	54.00 \pm 11.13	58.36 \pm 16.52
Sector 12	17.35 \pm 8.19	16.46 \pm 8.39	88.46 \pm 23.96	70.95 \pm 24.35

Data are expressed as the mean \pm SD

*Sector 9, 10: maculopapillary bundle, characterized by the absence of surface vessels in the area.

235

236

237

238

239

240 **Discussion**

241 The application of an early diagnosis of glaucoma and early intervention treatment plan,
242 without having to wait for clearly defined visual field losses, has led to the emergence of
243 a variety of types of new diagnostic imaging technology with the objective of measuring
244 structural changes which is very useful in glaucoma treatment [4-7].

245 In spite of all the studies that have attempted to confirm that the new imaging techniques
246 are good predictors of early structural glaucomatous damage, others question the ability
247 of these techniques [18–21].

248 There is no unanimous consensus on whether structural damage precedes functional
249 progression in glaucomatous eyes [22, 23]. It is probably caused by a definition problem
250 due to the limitation of instrumental capacity, specificity and sensitivity [24]. In addition,
251 we must not forget that we define and understand the term "early diagnosis" as the
252 presence of early signs of glaucoma, which in turn are characterized by being highly
253 variable and difficult to catalog [25]. In the clinical setting, we often find patients with
254 evidence of glaucomatous optic neuropathy without a detectable visual field abnormality,
255 patients with a glaucomatous visual field without detectable structural abnormality and
256 patients with a similar degree of stages of glaucomatous structural alterations but with
257 different levels of losses in the field visual [22]. Therefore, the diagnosis and monitoring
258 of glaucoma cannot be made based on a single examination.

259 We believe, like other researchers, that the problem really lies in the difficulty of the
260 concordance and relationship between the perception of the differential threshold
261 obtained by the visual field and the reduction of ganglion cells detected by the OCT [26].
262 The problem with all this lies in the fact that there is no linear relationship between the
263 measurements used in each test. The visual field uses logarithmic units of measurement,
264 decibels (dB), measuring the differential light sensitivity of the subject which are related

265 to the luminance of the stimulus relative to the background. Therefore, it does not express
266 the value of the detected luminosity as an absolute value but as a relative value. In
267 addition, OCT measures the thickness of peripapillary RNFL in linear units (μm) giving
268 a reference value with respect to normality measurements, as the μm is a linear unit which
269 has a direct measurement relationship with retinal ganglion cell density [22, 24].
270 It has been tried, without success, to create a model that relates both tests. Several authors
271 have attempted to do this, and even here there is still a diversity of opinions. Some believe
272 it is better to generate models whose association is considered more correct if both tests
273 are transferred to linear units [27] and others believe that, on the contrary, the association
274 is better if it is done in logarithmic units [29].
275 A possible solution and contribution, particularly for the improvement of lineal models,
276 is the model we propose in our study. We suggest determining a map in order to make up
277 for the lack of knowledge, which determines a relationship between structure and
278 functional damage in glaucoma, to match a bundle of nerve fibers of a certain region of
279 the retina examined by the visual field with the corresponding area of input of that bundle
280 of fibers in its corresponding sector in the ONH. In this way, we could obtain the thickness
281 of peripapillary nerve fibers measured by the OCT and the sensitivity values measured
282 by the visual field corresponding to each clock-hour sector. The best-considered and
283 most-used model for this is the Galway Heath (2000) [28] on which the Jansonius
284 retinotopic model (2009) [13] is based, and which we have used to generate our own
285 model. It differs from the rest by making a mathematical model mapping nerve fiber
286 bundle trajectories in the retina, describing a clear asymmetry between the superior and
287 inferior hemifields and providing a detailed location-specific estimate of the magnitude
288 of variability [14].
289

290 According to our data (Table 2), we can affirm that our model, which relates structural to
291 functional function, is reliable in trying to respond to the objective of this study since all
292 efforts are directed towards early detection of the disease in order to thus approaching it
293 with the most appropriate therapeutic considerations [25]. Reflection that leads us to ask
294 ourselves how to know that therapeutic action to apply is the correct one if the
295 etiopathogenesis of glaucoma is not really known. To resolve this question, after initially
296 programming our work methodology, we decided to clinically check one of the postulates
297 that this new theory defends [30,31]: if the blood vessel really has a protective role against
298 glaucomatous lesion both at the level of fiber thickness nerve as in light sensitivity values
299 in each of the 9 sections considered in the groups formed (group of subjects with
300 glaucoma in whose sections there is a presence of a vessel versus group of subjects with
301 glaucoma in whose sections there is no presence of a vessel) (Table 3). Note that the
302 sections in which we are going to find the position of a vessel will be section 1 and 7,
303 followed by section 2 and 6, respectively corresponding to the limiting region of the fibers
304 of the Bjerrum area and immediately more peripheral to these . In contrast, the sections
305 belonging to the papillo-macular bundle (sections 9, 10 and 11) are the most numerous in
306 the absence of a blood vessel.

307

308 **Conclusion**

309 In conclusion, we only found the protective role of a blood vessel was strongest for clock-
310 hour 12 on the thickness RFNL. We did not find an influence of the protective role of a
311 blood vessel for sensitivity values in any individual sector of the clock-hour map studied.
312 We cannot confirm that the blood vessel has a protective role against glaucomatous
313 damage based on the data obtained and we are not able to compare our results with those
314 obtained by other authors. To our knowledge, this is the first study that clinically proves

315 the protective role hypothesis of the blood vessel in glaucomatous damage and it supports
316 new theories that may determine the pathogenesis of glaucoma.

317 Based on these findings, additional studies are needed to evaluate the protective role of
318 the blood vessel applied to subjects with early glaucomatous damage, to check whether
319 there is a greater advance in the disease comparing those sectors with or without vascular
320 protection. It would also be interesting to study functionality by microperimetry which
321 has the capacity to detect minimum variations of the visual threshold in a more precise
322 way than the visual field.

323

324 **Abbreviations**

325 IOP: Intraocular pressure; ONH: Optic nerve head; POAG: Primary open angle
326 glaucoma; OCT: Optical coherence tomography; SD: Spectral domain; RNFL: Retinal
327 nerve fiber layer; NFL: Nerve fiber layer.

328

329 **Declarations**

330 **Availability of data and materials**

331 The datasets used and/or analyzed during the current study are available from the
332 corresponding author on reasonable request.

333 **Conflicts of interests**

334 The authors declares that there is no conflict of interest regarding the publication of this
335 article.

336 **Funding Statement**

337 No funding was received for this research.

338 **Acknowledgements**

339 Not applicable.

340 **Authors' contributions**

341 YC: data acquisition and analysis, interpretation of data, drafting the manuscript and
342 critical revision of the manuscript. JL: research design and critical revision of the
343 manuscript. LV, MR, JL: critical revision of the manuscript. RL: analysis and
344 interpretation of data. All authors have read and approved the manuscript.

345 **Approved by the following research ethics committee:**

346 This study was approved by the Ethics Committee of the Catholic University of Murcia
347 (CE041809). The present investigation was conducted according to the tenets of the
348 Declaration of Helsinki and current regulations to protect the confidentiality of data. The
349 research is based entirely on the clinical routine and is obtained from the patient's medical
350 record system. Therefore, no informed consent is required.

351 **Consent for publication**

352 Not applicable

353

354 **References**

355 Referencias

356

357 1. Actis AG, Versino E, Brogliatti B, Rolle T. Risk Factors for Primary Open Angle
358 Glaucoma (POAG) Progression: A Study Ruled in Torino. *Open Ophthalmol J.* 2016;
359 10:129-139.

360

361 2. Levin LA. Pathophysiology of the progressive optic neuropathy of glaucoma.
362 *Ophthalmol Clin North Am.* 2005; 18(3): 355-364.

363

364 3. Carreras FJ. Pathogenesis of glaucoma: how to prevent ganglion cell from axonal
365 destruction?. *Neural Regen Res.* 2014; 9(23): 2046-2047.

366

367 4. Park SB, Sung KR, Kang SY, Kim KR, Kook MS. Comparison of glaucoma diagnostic
368 capabilities of cirrus HD and Stratus optical coherence tomography. *Arch Ophthalmol.*
369 2009;127(12):1603-1609./

370

371 5. Mwanza JC, Oakley JD, Budenz DL, Anderson DR. Ability of cirrus HD-OCT optic
372 nerve head parameters to discriminate normal from glaucomatous eyes. *Ophthalmology.*
373 2011; 118(2): 241-248.

374

- 375 6. Lisboa R, Paranhos A Jr, Weinreb RN, Zangwill LM, Leite MT, Medeiros FA.
376 Comparison of different spectral domain OCT scanning protocols for diagnosing
377 preperimetric glaucoma. *Invest Ophthalmol Vis Sci.* 2013; 54(5): 3417-3425.
378
- 379 7. Leal-Fonseca M, Rebolleda G, Oblanca N, Moreno-Montañes J, Muñoz-Negrete FJ.
380 A comparison of false positives in retinal nerve fiber layer, optic nerve head and macular
381 ganglion cell-inner plexiform layer from two spectral-domain optical coherence
382 tomography devices. *Graefes Arch Clin Exp Ophthalmol.* 2014; 252(2): 321-330.
383
- 384 8. Alasil T, Wang K, Yu F, Field MG, Lee H, Baniasadi N et al. Correlation of retinal
385 nerve fiber layer thickness and visual fields in glaucoma: a broken stick. *Am J*
386 *Ophthalmol.* 2014;157(5):953-959
387
- 388 9. Carreras FJ, Porcel D, Muñoz-Avila JI. Mapping the Surface astrocytes of the optic
389 disc: a fluid-conducting role of the astrocytic covering of the central vessels. *Clin Exp*
390 *Ophthalmol.* 2010; 38(3): 300-308.
391
- 392 10. Wolter JR. Pores in the internal limiting membrane of the human retina. *Acta*
393 *Ophthalmol Scand.* 1994; 42: 971-974.
394
- 395 11. Carreras FJ, Porcel D, Guerra-Tschuschke I, Carreras I. Fenestrations and preferential
396 flow routes in the prelaminar optic nerve through wet scanning electron microscope and
397 perfusion of tracers. *Clin Exp Ophthalmol.* 2010; 38(7): 705-717.
398
- 399 12. Carreras FJ, Porcel D, Alaminos M, Garzon I. Cell-cell adhesion in the prelaminar
400 region of the optic nerve head: a possible target for ionic stress. *Ophthalmic Res.* 2009;
401 42(2): 106-111.
402
- 403 13. Jansonius NM, Nevalainen J, Selig B, Zangwill LM, Sample PA, Budde WM et al. A
404 mathematical description of nerve fiber bundle trajectories and their variability in the
405 human retina. *Vision Res.* 2009; 49(17): 2157-2163.
406
- 407 14. Jansonius NM, Schiefer J, Nevalainen J, Paetzold J, Schiefer U. A mathematical
408 model for describing the retinal nerve fiber bundle trajectories in the human eye: average
409 course, variability, and influence of refraction, optic disc size and optic disc position. *Exp*
410 *Eye Res.* 2012; 105: 70-78.
411
- 412 15. Ferreras A, Pablo LE, Garway-Heath DF, Fogagnolo P, García-Feijoo J. Mapping
413 standard automated perimetry to the peripapillary retinal nerve fiber layer in glaucoma.
414 *Invest Ophthalmol Vis Sci.* 2008; 49(7): 3018-3025.
415
- 416 16. Wollstein G, Ishikawa H, Wang J, Beaton SA, Schuman JS. Comparison of three
417 optical coherence tomography scanning areas for detection of glaucomatous damage. *Am*
418 *J Ophthalmol.* 2005; 139(1): 39-43.
419
- 420 17. Garcia-Medina JJ, Garcia Medina M, Zanon-442 Moreno V, Garcia-Maturana C,
421 Cruz-Espinosa FJ, Pinazo-Duran MD. Comparison of global indices and test duration
422 between two visual field analyzers: Octopus 300 and Topcon SBP-3000. *Graefes Arch*
423 *Clin Exp Ophthalmol.* 2012; 250(9): 1347-1351.
424

- 425
426 18. Hougaard JL, Heijl A, Bengtsson B. Glaucomatous retinal nerve fiber layer defects
427 may be identified in Stratus OCT images classified as normal. *Acta Ophthalmol.* 2008;
428 86(5): 569-575.
429
430 19. Pantcheva MB, Wollstein G, Ishikawa H, Noecker RJ, Schuman JS. Optical
431 coherence tomography algorithm failure to detect nerve fiber layer defects: report of two
432 cases. *Br J Ophthalmol.* 2009; 93(9): 1141-1142.
433
434 20. Hwang YH, Kim YY, Kim HK, Sohn YH. Ability of cirrus high-definition spectral
435 domain optical coherence tomography clock-hour, deviation, and thickness maps in
436 detecting photographic retinal nerve fiber layer abnormalities. *Ophthalmology.* 2013;
437 120(7): 1380-1387.
438
439 21. Rao HL, Addepalli UK, Chaudhary S, Kumbar T, 393 Senthil S, Choudhari NS,
440 Garudadri CS. Ability of different scanning protocols of spectral domain optical
441 coherence tomography to diagnose preperimetric glaucoma. *Invest Ophthalmol Vis Sci.*
442 2013;54(12): 7252-7257.
443
444 22. Malik R, Swanson WH, Garway-Heath DF. Structure-function relationship in
445 glaucoma: past thinking and current concepts. *Clin Experiment Ophthalmol.* 2012;
446 40(4):369-380.
447
448 23. Öhnell H, Heijl A, Anderson H, Bengtsson B. Detection of glaucoma progression by
449 perimetry and optic disc photography at different stages of the disease: results from the
450 Early Manifest Glaucoma Trial. *Acta Ophthalmol.* 2017; 95(3): 281-287.
451
452
453 24. Hood DC, Kardon RH. A framework for comparing structural and functional
454 measures of glaucomatous damage. *Prog Retin Eye Res.* 2007; 26(6): 688-710.
455
456 25. Chauhan BC. Detection of glaucoma: the role of new functional and structural tests.
457 410 *Curr Opin Ophthalmol.* 2004; 15(2): 93-95.
458 26. Anderson RS. The psychophysics of glaucoma: improving the structure/function
459 relationship. *Prog Retin Eye Res.* 2006; 25(1): 79-97.
460
461 27. Bowd C, Zangwill LM, Medeiros FA, Tavares IM, Hoffmann EM, Bourne RR,
462 Sample PA, Weinreb RN. Structure-function relationships using confocal scanning laser
463 ophthalmoscopy, optical coherence tomography, and scanning laser polarimetry. *Invest*
464 *Ophthalmol Vis Sci.* 2006; 47(7): 2889-2895.
465
466 28. Garway-Heath DF, Poinoosawmy D, Fitzke FW, Hitchings RA. Mapping the visual
467 field to the optic disc in normal tension glaucoma eyes. *Ophthalmology.* 2000; 107(10):
468 1809-1815.
469
470 29. Leung CK, Chong KK, Chan WM, Yiu CK, Tso MY, Woo J, Tsang MK, Tse KK,
471 Yung WH. Comparative study of retinal nerve fiber layer measurement by Stratus OCT
472 and GDx VCC, II: structure/function regression analysis in glaucoma. *Invest Ophthalmol*
473 *Vis Sci.* 2005; 46(10): 3702-3711.
474

- 475 30. Carreras FJ, Rica R, Delgado AV. Modeling the patterns of visual field loss in
476 glaucoma. *Optom Vis.* 2011; 88(1): E63-79.
477 31. Carreras FJ, Medina J, Ruiz-Lozano M, Carreras I, Castro JL. Virtual tissue
478 engineering and optic pathways: plotting the course of the axons in the retinal nerve fiber
479 layer. *Invest Ophthalmol Vis Sci.* 2014; 55(5): 3107-3119.
480

481 **Additional file**

- 482 STROBE Statement—Checklist of items that should be included in reports of *cross-sectional*
483 *studies*

	Item No	Recommendation
Title and abstract	1	(a) Indicate the study’s design with a commonly used term in the title or the abstract: <i>“Title, page 2”</i> (b) Provide in the abstract an informative and balanced summary of what was done and what was found: <i>“Abstract, paragraph 2,3”</i>
Introduction		
Background/rationale	2	Explain the scientific background and rationale for the investigation being reported: <i>“Background, paragraph 2,3,”</i>
Objectives	3	State specific objectives, including any prespecified hypotheses: <i>“Background, Paragraph 4,5”</i>
Methods		
Study design	4	Present key elements of study design early in the paper: <i>“Methods, paragraph 1”</i>
Setting	5	Describe the setting, locations, and relevant dates, including periods of recruitment, exposure, follow-up, and data collection: <i>“Methods, paragraph 1”</i>
Participants	6	(a) Give the eligibility criteria, and the sources and methods of selection of participants: <i>“Methods, paragraph 3”</i>
Variables	7	Clearly define all outcomes, exposures, predictors, potential confounders, and effect modifiers. Give diagnostic criteria, if applicable
Data sources/ measurement	8*	For each variable of interest, give sources of data and details of methods of assessment (measurement). Describe comparability of assessment methods if there is more than one group
Bias	9	Describe any efforts to address potential sources of bias: <i>“N/A”</i>
Study size	10	Explain how the study size was arrived at: <i>“N/A”</i>
Quantitative variables	11	Explain how quantitative variables were handled in the analyses. If applicable, describe which groupings were chosen and why: <i>“N/A”</i>
Statistical methods	12	(a) Describe all statistical methods, including those used to control for confounding (b) Describe any methods used to examine subgroups and interactions: <i>“N/A”</i> (c) Explain how missing data were addressed: <i>“N/A”</i> (d) If applicable, describe analytical methods taking account of sampling strategy: <i>“N/A”</i> (e) Describe any sensitivity analyses: <i>“N/A”</i>
Results		
Participants	13*	(a) Report numbers of individuals at each stage of study—eg numbers potentially eligible, examined for eligibility, confirmed

		eligible, included in the study, completing follow-up, and analysed: <i>"Results, paragraph 1"</i>
		(b) Give reasons for non-participation at each stage: <i>"Results, paragraph 1"</i>
		(c) Consider use of a flow diagram: <i>"N/A"</i>
Descriptive data	14*	(a) Give characteristics of study participants (eg demographic, clinical, social) and information on exposures and potential confounders: <i>"N/A"</i> (b) Indicate number of participants with missing data for each variable of interest: <i>"N/A"</i>
Outcome data	15*	Report numbers of outcome events or summary measures: <i>"Results, paragraph 1"</i>
Main results	16	(a) Give unadjusted estimates and, if applicable, confounder-adjusted estimates and their precision (eg, 95% confidence interval). Make clear which confounders were adjusted for and why they were included: <i>"N/A"</i> (b) Report category boundaries when continuous variables were categorized: <i>"N/A"</i> (c) If relevant, consider translating estimates of relative risk into absolute risk for a meaningful time period: <i>"N/A"</i>
Other analyses	17	Report other analyses done—eg analyses of subgroups and interactions, and sensitivity analyses: <i>"N/A"</i>
Discussion		
Key results	18	Summarise key results with reference to study objectives: <i>"Conclusion, paragraph 1"</i>
Limitations	19	Discuss limitations of the study, taking into account sources of potential bias or imprecision. Discuss both direction and magnitude of any potential bias: <i>"Conclusion, paragraph 2"</i>
Interpretation	20	Give a cautious overall interpretation of results considering objectives, limitations, multiplicity of analyses, results from similar studies, and other relevant evidence: <i>"Conclusion, paragraph 1"</i>
Generalisability	21	Discuss the generalisability (external validity) of the study results. <i>"Conclusion, paragraph 1"</i>
Other information		
Funding	22	Give the source of funding and the role of the funders for the present study and, if applicable, for the original study on which the present article is based: <i>"N/A"</i>